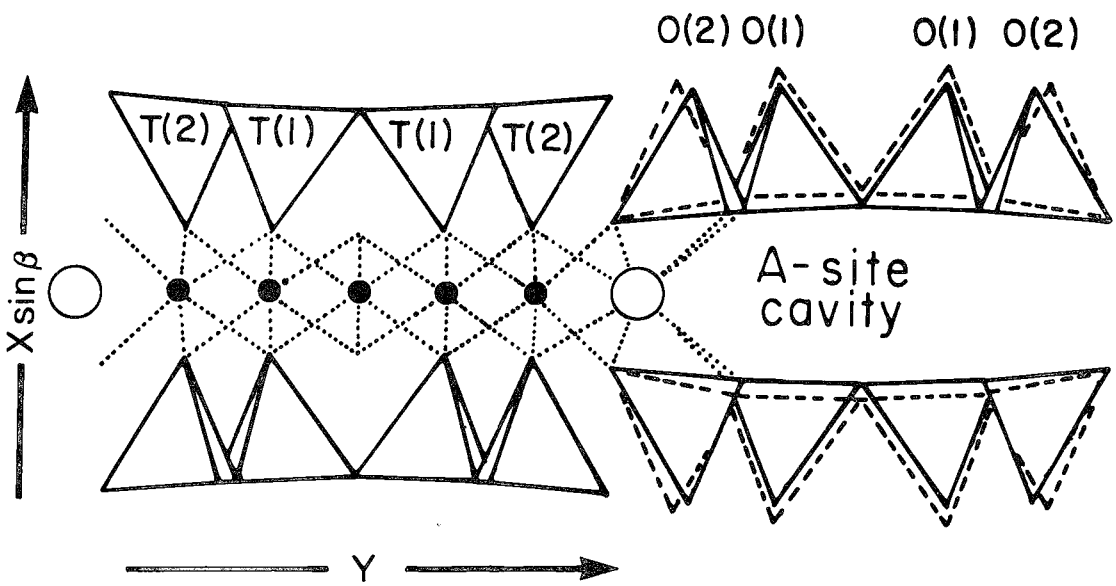

FIG. 108. The room-temperature crystal structure of tremolite projected down *Z*. The dashed lines associated with the tetrahedral double-chains show their movement (highly exaggerated) with increasing temperature [after Sueno *et al.* (1973)].

In tremolite, the increase in equivalent isotropic temperature-factors for all ions at all sites is linear with temperature (Sueno *et al.* 1973). The observed values and the rates of increase are approximately the same for identical cations (Table 67), and seem to be inversely related to the mean bond-valence in the co-ordination polyhedron. For the anions, both the magnitudes and the rates of increase with temperature are inversely related to the co-ordination number of the anion. The overall behavior of the thermal vibration model of tremolite is very similar to that of diopside (Cameron & Papike 1981).

TABLE 67. VARIATION OF EQUIVALENT ISOTROPIC TEMPERATURE FACTORS (Å^2) WITH TEMPERATURE DERIVED FROM HIGH-TEMPERATURE CRYSTAL-STRUCTURE REFINEMENTS

	Tremolite				Tirodite		
	(30)	(56a)	(56b)		($\bar{2}7$)	(41)	
	24°C	400°C	700°C	C.N.	24°C	270°C	C.N.
O(1)	0.35(3)	1.02(4)	1.49(6)	4	0.41	1.07(6)	4
O(2)	0.39(3)	1.06(4)	1.52(6)	4	0.46	0.97(6)	4
O(3)	0.46(4)	1.26(6)	1.79(8)	3	0.48	0.93(8)	3
O(4)	0.51(3)	1.42(5)	2.02(6)	3	0.67	1.50(7)	3
O(5)	0.46(3)	1.26(5)	1.88(6)	3	0.60	1.37(3)	2,3
O(6)	0.45(3)	1.29(5)	1.81(6)	3	0.89	1.46(7)	3
O(7)	0.50(4)	1.39(7)	2.18(9)	2	0.89	1.34(9)	2
T(1)	0.19(1)	0.77(2)	1.07(3)	4	0.27	0.78(2)	4
T(2)	0.19(1)	0.77(2)	1.11(3)	4	0.30	0.88(2)	4
M(1)	0.33(2)	1.02(3)	1.38(4)	6	0.38	0.89(4)	6
M(2)	0.31(2)	0.95(3)	1.38(4)	6	0.37	1.00(4)	6
M(2)	0.33(2)	0.97(4)	1.34(5)	6	0.36	0.96(6)	6
M(4)	0.57(1)	1.53(2)	2.27(4)	8	0.95	1.36(3)	6,8

ELECTRICAL PROPERTIES OF AMPHIBOLES

The electrical properties of a mineral govern its behavior in an applied electric field. The two main electrical properties are the *resistivity*, the reciprocal of the conductivity, which is a measure of the conduction current developed by an electric field, and the *dielectric constant*, a measure of the electrical polarization that occurs in an applied electrical field. There are very few studies of the electrical properties of amphiboles. Littler & Williams (1965) measured the conductivity of crocidolite along the fibre direction as a function of temperature. Typical results are summarized in Figure 109. Progressive oxidation resulted in systematically different behavior in repeated experiments; activation energies for conduction are 0.69(4) and 0.33(4) eV, respectively. Specific resistances for three samples were 10^9 ohm cm^{-1} for two samples of iron-rich crocidolite and 10^{10} ohm cm^{-1} for an iron-poor crocidolite. Conductivity across the fibre direction was found to be very low. Tolland (1973) performed similar experiments on a "hornblende" with an Fe/(Fe+Mg) ratio of ~0.19. The results are summarized in Figure 109; the activation energies found were 0.54 eV along *Z* and 0.57 eV along *Y*. Both studies suggested the conduction mechanism in amphiboles to be the electron-hopping process

$$Fe^{3+} + e^- \rightleftharpoons Fe^{2+}.$$

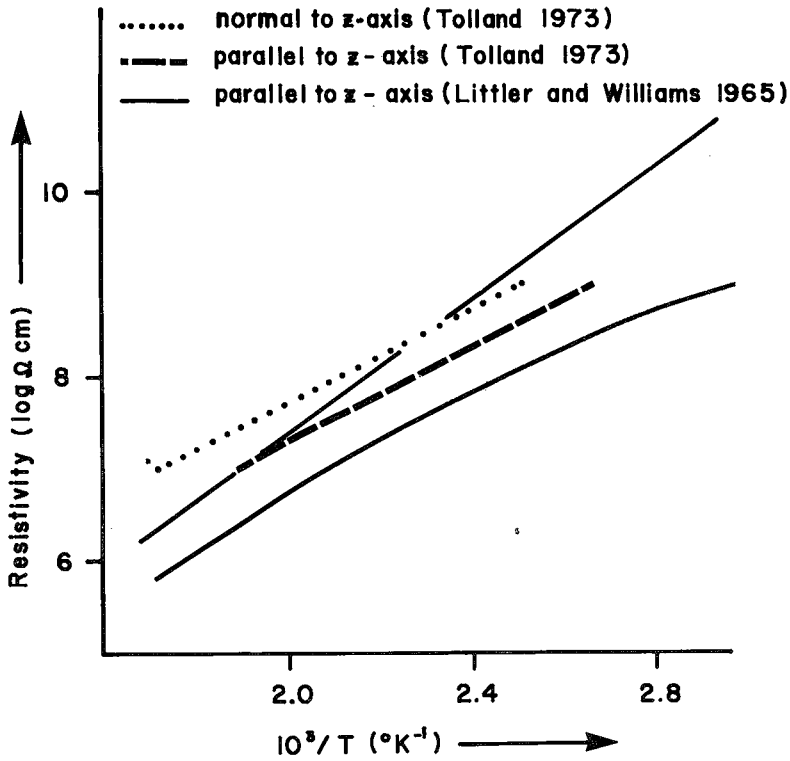

FIG. 109. Variation in resistivity with temperature in single crystals of amphibole; for crocidolite (Littler & Williams 1965), the linear relationship is for an initial heating experiment, the nonlinear relationship is for the fifth cycle of heating; data for "amphibole" are from Tolland (1973).

Keller (1966) gave in graphical form the variation of resistivity with frequency at several different temperatures for "actinolite rock" (Fig. 110); the resistivity decreases with rising temperature. At low temperatures, the resistivity is inversely correlated with frequency; with increasing temperature, this dependence decreases until at ~1000°C, the resistivity is independent of frequency. The actinolite will probably have broken down long before this stage is reached; in fact, a lot of the data here will have been recorded after the amphibole has exceeded its maximum thermal stability limit and has broken down. However, in the absence of any compositional data on the "actinolite", it is difficult to estimate at what temperature this would have occurred.

Vijayasree *et al.* (1976) studied the variation in frequency of the dielectric constant and the dielectric loss of fibrous tremolite with varying temperature; a graphical summary of their results is shown in Figure 111. There is a marked variation of dielectric constant in the lower-frequency range at room temperature, but the general pattern for the high-temperature measurements is the same, a very slight decrease in dielectric constant with increasing frequency. There is a minimum in the dielectric constants at ~660°C (see Fig. 111b) and a maximum at ~850°C. This behavior is indicative of amphibole breakdown (Vijayasree *et al.* 1976), the rapid fall of the dielectric-loss data (Figs. 111c and 111d) above ~800°C being associated with the structural transformation.

MAGNETIC PROPERTIES OF AMPHIBOLES

There has been considerable interest in the magnetic susceptibility of amphiboles. The first extensive investigation was that of Syono (1960), who measured the magnetization curves at room temperature and low temperature, and the variation of magnetic susceptibility with temperature for six chemically analyzed clinoamphiboles. Similar studies have been carried out by Babkine *et al.* (1968) and Efimov *et al.*

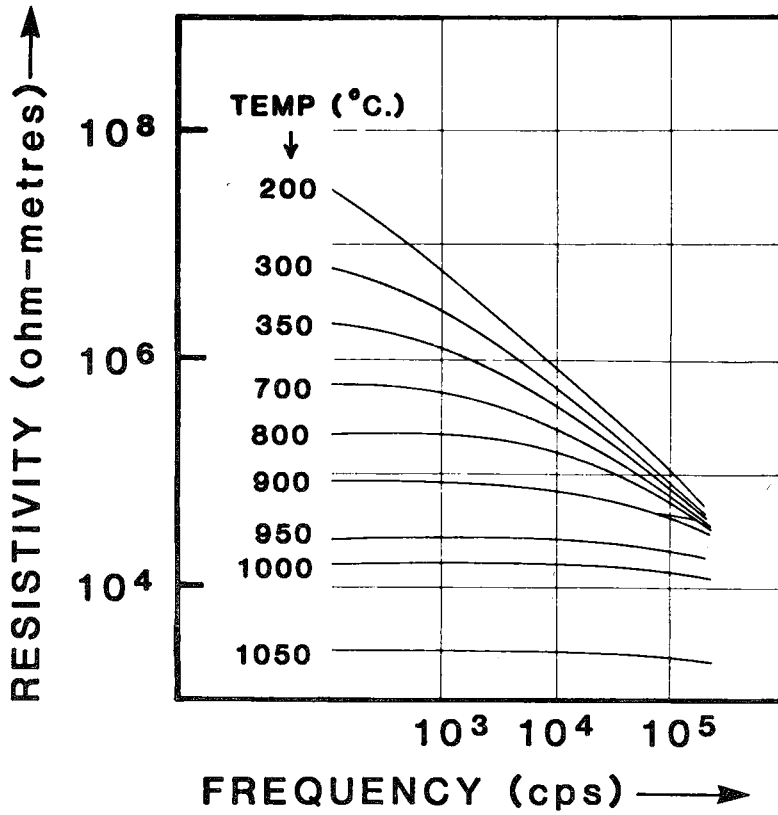

FIG. 110. Variation in resistivity with frequency for "actinolite rock" at several different temperatures [from Keller (1966)].

(1972). The chemistry of the amphiboles and the relevant magnetic data are given in Appendix H. A brief review and discussion of magnetic properties of paramagnetic minerals in general (including amphiboles) are given by Parks & Akhtar (1968). Most authors have compared their experimental values of magnetic susceptibility with theoretical values calculated from Langevin's formula (Kittel 1966), and have noted that the measured values are larger than the calculated values by ~25%. Syono (1960) has noted that minerals containing H_2O or OH (or both) commonly show this behavior. However, Parks & Akhtar (1968) noted that the pyroxenes also show this behavior, and suggested that it is due to "crystal-field effects".

The magnetic behavior of amphiboles has also been investigated by Mössbauer spectroscopy, in which low-temperature experiments have shown the presence of magnetic ordering. Magnetic hyperfine splitting was first observed in amphiboles by Buckley & Wilkins (1971) for cummingtonite{62}; they recorded the spectrum at 4.2 K and obtained a reasonable fit using nine peaks (Fig. 112), although they suggested that this was of "limited significance". These authors also noted that the spectrum at 55 K was not appreciably different from the spectrum at 78 K, indicating the cummingtonite to be magnetically disordered at these temperatures. Borg & Borg (1974) have shown the presence of hyperfine splitting in the 4.2 K spectrum of crossite{17a}, manganoan riebeckite{79} and arfvedsonite{80}, and have determined the temperature at which the onset of magnetic ordering occurs in each of these amphiboles. The Mössbauer and magnetic-hyperfine-splitting parameters are shown in Table 68. Borg *et al.* (1975) reported high-field magnetization and susceptibility measurements on arfvedsonite{80}. The temperature dependence of the magnetic susceptibility is shown in Figure 113; there is an obvious transition at 31.5 K that may be ascribed to antiferromagnetic order. Figure 114 shows the magnetization as a function of the applied field for several different temperatures

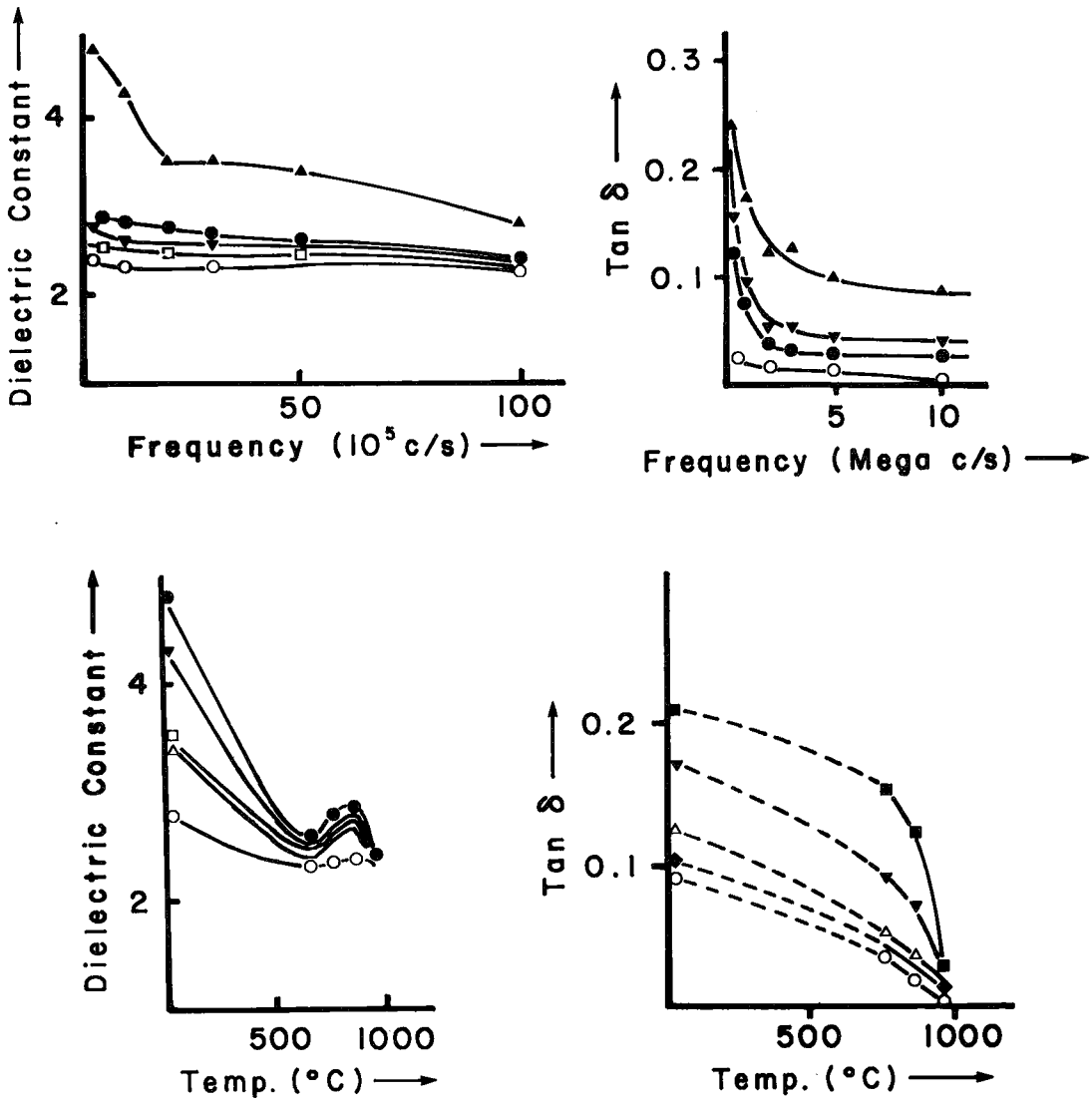

FIG. 111. Dielectric properties of fibrous tremolite; (a) variation of dielectric constant with frequency at various temperatures; (b) variation of dielectric constant with temperature at different frequencies; (c) variation of dielectric loss (tan δ) with frequency at different temperatures; (d) variation of dielectric loss with temperature at different frequencies. For clarity, some data-points have been omitteed from each diagram [after Vijayasree *et al.* (1976)].

with $\vec{H}//Z$. The magnetization passes through zero for all temperatures, as is appropriate for antiferromagnetic order. However, it is not apparent whether the magnetic order within each chain is predominantly antiferromagnetic or whether it is ferromagnetic with antiferromagnetic coupling between chains. Borg & Borg (1980) reported on this work in more detail, giving additional results, including both powder and single-crystal magnetic hyperfine spectra. The magnetic hyperfine spectra for arfvedsonite {80} are shown in Figure 115; the spectra consist of an overlap of three separate six-line spectra due, respectively, to Fe^{3+} at M(2), Fe^{2+} at M(1) and Fe^{2+} at M(3). As the values of the magnetic hyperfine splitting for Fe^{2+} and Fe^{3+} are distinctly different ($\sim$10–11 mm/s and 16–18 mm/s, respectively), the outermost pair

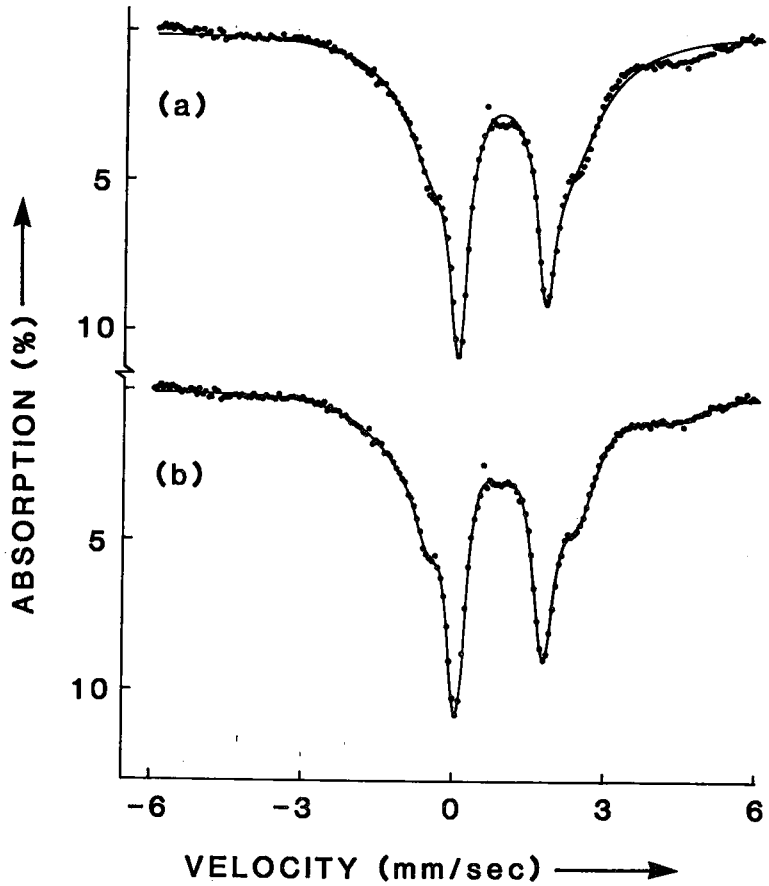

FIG. 112. Mössbauer spectrum of cummingtonite{62} at liquid helium (4.2 K) temperatures; upper: spectrum fit to four Lorentzian peaks; lower: spectrum fit to nine Lorentzian peaks [from Buckley & Wilkins (1971)].

of peaks can be assigned to Fe^{3+} at M(2) only, with the remainder of the spectrum being a *mélange* of 4 Fe^{3+} peaks and 12 Fe^{2+} peaks. This resolution of the Fe^{3+} peaks allowed the determination of the orientation of the Fe^{3+} magnetic moment from single-crystal spectra. The direction established was ~//[316], and Borg & Borg (1980) suggested that the Fe^{2+} magnetic moment is also parallel to this direction. The antiferromagnetic character and the orientation of the magnetic moment indicate that there are coupling interactions between the octahedral strips in the structure.

Eisenstein *et al.* (1975) examined two virtually uncharacterized amphiboles, designated "amosite" and "crocidolite", using magnetic susceptibility, electron-spin-resonance and Mössbauer-spectroscopic methods, and presented a brief survey of their results for amosite. At 30 K this particular "amosite" has a paramagnetic spectrum; in the 15 K Mössbauer spectrum,

TABLE 68. MÖSSBAUER AND MAGNETIC HYPERFINE SPLITTING PARAMETERS (Fe^{3+}) IN AMPHIBOLES

	{17a}	{79}	{80}
Magnetic ordering temperature (K)	6.2	22.5	26.0
Q.S. (mm/s)	0.22	0.32	0.31
I.S. (mm/s)	-0.848	-0.968	-0.993
Magnetic hyperfine splitting	17.55*	17.66	17.53

*this value measured at 2.67 K; all other values at 4.6 K. Data from Borg & Borg (1974).

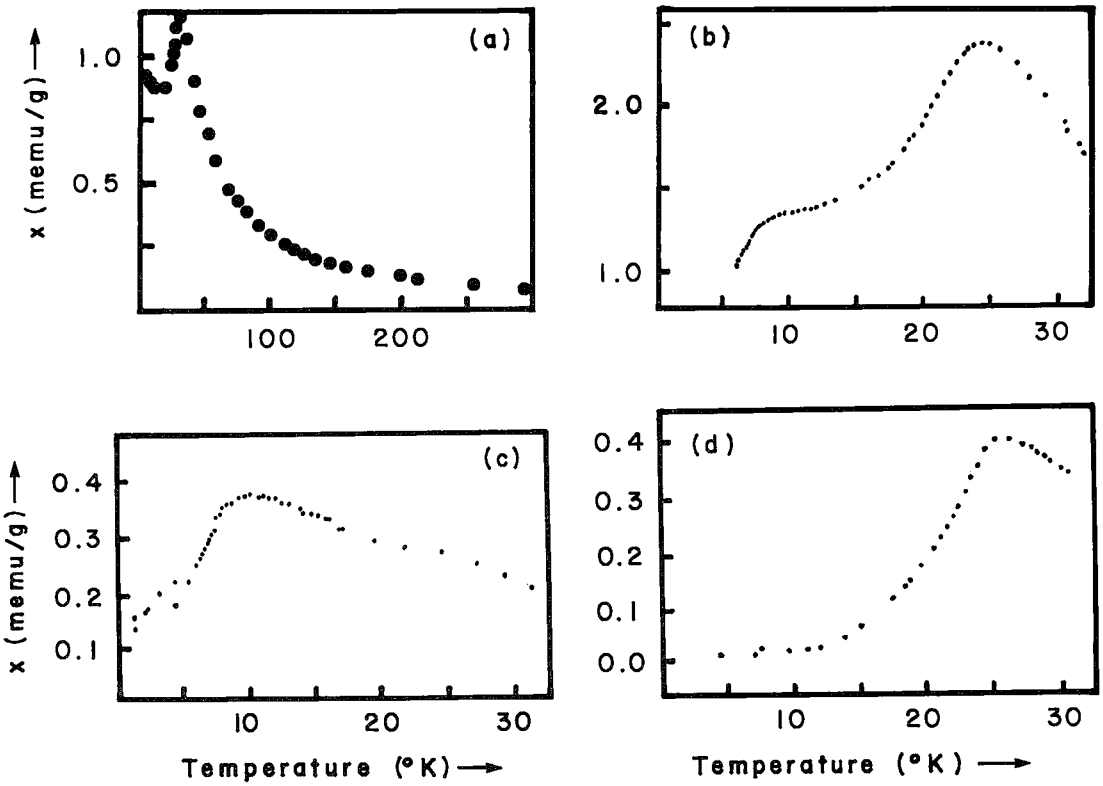

FIG. 113. Magnetic susceptibility as a function of temperature: (a) powdered arfvedsonite{80}, from Borg *et al.* (1975); (b) powdered amosite; (c) amosite fibre bundle, //*Z* axis; (d) amosite fibre bundle, $\perp$ *Z* axis [(b), (c) and (d) from Eisenstein *et al.* (1975)].

the M(1) + M(2) + M(3) doublet is discernible but broadened slightly, whereas in place of the M(4) doublet is a broad magnetic hyperfine structure; the magnetic hyperfine structure is better developed in the 11 K spectrum, and in the 4.2 K spectrum, both groups of cations, the M(4) and the M(1) + M(2) + M(3) groups, show magnetic hyperfine structure. Clearly the Mössbauer results of this study are not similar to those of Buckley & Wilkins (1971). The electron-spin-resonance experiment confirmed the lack of Fe^{3+} in the structure. The powder magnetic susceptibility was measured from 1 to 30 K on randomly oriented samples and on samples of parallel aggregates of fibres both parallel and perpendicular to the fibre axes; the results are shown in Figure 113. There are two peaks in the powder susceptibility data, one at 25 K and the other at 10 K. Correlating the Mössbauer and magnetic susceptibility results, Eisenstein *et al.* (1975) suggested that Fe^{2+} at the M(4) sites orders antiferromagnetically below 25 K, and Fe^{2+} at M(1) + M(2) + M(3) orders antiferromagnetically below 10 K.

Elastic Properties of Amphiboles

In a crystalline solid, there are, in principle, nine stress components X_{pq}, and linearly dependent on these are nine strain components e_{rs}. Stress and strain are thus connected by a fourth-rank tensor:

$$X_{pq} = C_{rspq}e_{rs}$$

where C are the elastic stiffness constants (moduli of elasticity), and:

$$e_{rs} = S_{pqrs}X_{pq}$$

where S are the elastic compliance constants (elastic constants). Imposing the condition that the angular acceleration of the crystal vanishes, the number of independent stress-components is reduced from nine to six and the number of non-zero tensor components is reduced to thirty-six. In the approximation of Hooke's law,

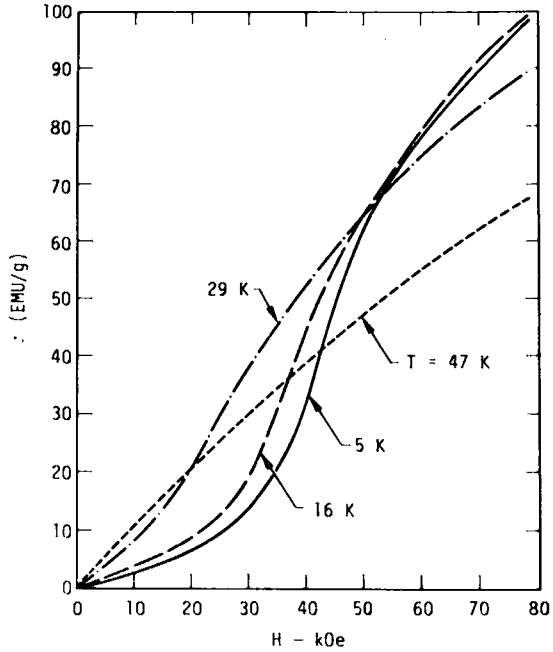

FIG. 114. Dependence of magnetization σ on the applied field, H at several different temperatures, with the field //Z, for arfvedsonite{80} [from Borg & Borg (1980)].

the elastic-energy density U of a crystal is a quadratic function of the strains (Kittel 1966); thus

$$U = 1/2 \sum_{i=1}^{6} \sum_{j=1}^{6} \tilde{C}_{ij} e_i e_j$$

where the indices $1 \rightarrow 6$ are defined as:

$1 \equiv 11; 2 \equiv 22; 3 \equiv 33; 4 \equiv 23; 5 \equiv 31; 6 \equiv 12.$

The stress components are found from the first derivative of U with respect to the associated component of strain:

$$X_i = \frac{\partial U}{\partial e_{ii}} \cdot \frac{\partial U}{\partial e_i} = \tilde{C}_{ii} e_i + 1/2 \sum_{\substack{j=1 \\ j \neq i}}^{6} (\tilde{C}_{ij} + \tilde{C}_{ji}) e_j.$$

As only the combination ½ $(\tilde{C}_{ij} + \tilde{C}_{ji})$ enters the stress–strain relationship, the elastic stiffness constants must be symmetrical:

$$C_{ij} = 1/2(\tilde{C}_{ij} + \tilde{C}_{ji}) = C_{ji}.$$

Thus the thirty-six elastic-stiffness constants are reduced to twenty-one. The presence of crystallographic symmetry requires that the elastic-energy density U be invariant under all symmetry operations of the relevant point-group. Thus for the clinoamphiboles

$$C_{14} = C_{16} = C_{24} = C_{26} = C_{34} = C_{36} = C_{45} = C_{56} = 0$$

leaving thirteen unique nonzero elastic-stiffness constants. The only detailed work on the amphiboles is that of Aleksandrov & Ryzhova (1961), who determined the elastic properties of two "hornblendes". The data are presented in Table 69, together with the available mineralogical data for the amphiboles used in the work. The moduli of elasticity C_{11}, C_{22} and C_{33} represent pure compression // X^*, Y and Z, respectively. In both examples, C_{11} is significantly less than C_{22} and C_{33}, indicating that the structures are most easily compressed along X^*. Examination of Figure 9 suggests that this may be the result of compression of the A-site cavity along X^* with the I-beam units themselves compressing much less. If this is the case, one might expect considerable variations in C_{11} throughout the amphiboles, depending on whether or not the A site is occupied. C_{44}, C_{55} and C_{66} are pure-shear moduli // YZ, X^*Z and X^*Y, respectively. In both samples, C_{44} is significantly greater than C_{55} and C_{66}, indicating more resistance to shear in the YZ plane than in the other planes.

The early work of Adams & Williamson (1923) has been summarized by Birch (1966): for the expression $\Delta V/V = aP$ (where V = volume, ΔV = change in volume, P = pressure in megabars), hornblende has the value a in the range 1.1 – 1.2, and actinolitic amphibole has the value $a = 1.3$, which is the mean value over a range from 2 to 12 kbar.

DEFORMATION BEHAVIOR OF AMPHIBOLES

Deformation behavior of nonasbestiform amphiboles in natural rocks is generally of the brittle type, although ductile deformation can occur (Gavasci 1973). In most tectonites, where most of the constituent minerals show ductile